

Extraction of Fetal Electrocardiogram by Combining Deep Learning and SVD-ICA-NMF Methods

Said Ziani*, Yousef Farhaoui, and Mohammed Moutaib

Abstract: This paper deals with detecting fetal electrocardiogram FECG signals from single-channel abdominal lead. It is based on the Convolutional Neural Network (CNN) combined with advanced mathematical methods, such as Independent Component Analysis (ICA), Singular Value Decomposition (SVD), and a dimension-reduction technique like Nonnegative Matrix Factorization (NMF). Due to the highly disproportionate frequency of the fetus's heart rate compared to the mother's, the time-scale representation clearly distinguishes the fetal electrical activity in terms of energy. Furthermore, we can disentangle the various components of fetal ECG, which serve as inputs to the CNN model to optimize the actual FECG signal, denoted by FECGr, which is recovered using the SVD-ICA process. The findings demonstrate the efficiency of this innovative approach, which may be deployed in real-time.

Key words: fetal electrocardiogram; Convolutional Neural Network (CNN); Deep Learning (DL); feature extraction

1 Introduction

In recent years, a new vocabulary related to the advent of artificial intelligence in our society has invaded scientific literature. We frequently refer to allied technologies such as deep learning when discussing artificial intelligence. Deep Learning (DL) is an algorithm that simulates the human brain's operations using artificial neural networks. Networks are composed of countless layers of neurons, each receiving and interpreting information from the layer beneath it. Deep learning models tend to function well with vast volumes of data,

but more conventional machine learning models cease to improve after reaching a point of data saturation. With the advent of big data and ever-more-powerful computing components, power and data-intensive, deep learning algorithms have outpaced the majority of previous approaches over time. They appear capable of resolving many health issues physicians encounter, particularly the interpretation of biological signals ECG, EMG, and EEG. In this paper, we will focus on one of the most powerful algorithms of DL^[1,2] and the Convolutional Neural Network (CNN)^[3,4]. CNNs are powerful programming models that allow the recognition of images by automatically assigning a label corresponding to the image's class membership to each image provided as input. Today, more than 17 million people die of cardiovascular disease yearly, according to the World Health Organization (WHO). In Morocco, cardiovascular diseases are the leading cause of death. A heart defect can occur from the first days of pregnancy, so vigilance must be increased, and close monitoring of any newborn is necessary. Whether inherited or not, congenital heart disease varies, while remission depends on early diagnosis. Each year in Morocco, an average of 6000 newborns suffer from a heart defect or congenital heart disease. Prenatal

• Said Ziani is with the Research Group in Biomedical Engineering and Pharmaceutical Sciences, ENSAM, Mohammed V University, Rabat 10090, Morocco, and the High School of Technology ESTC, University of Hassan II, Casablanca 20153, Morocco. E-mail: ziani9@yahoo.fr.

• Yousef Farhaoui is with the STI Laboratory, T-IDMS, Faculty of Sciences and Techniques, Moulay Ismail University of Meknes, Errachidia 52000, Morocco. E-mail: y.farhaoui@fste.umi.ac.ma.

• Mohammed Moutaib is with the IMAGE Laboratory, University of Moulay Ismail, Meknes 50000, Morocco. E-mail: mohammed.93@live.fr.

* To whom correspondence should be addressed.

Manuscript received: 2022-08-28; revised: 2022-09-19; accepted: 2022-09-27

pathology is often diagnosed at the onset of symptoms in infants. According to specialists, early diagnosis, that is, before birth or from the first weeks of pregnancy, is made relatively late in Morocco. It is from there that our scientific contribution will present a solution that sets up a reliable tool capable of early detection of heart defects: the Fetal ECG (FECG). FECG can be monitored by placing electrodes on the mother's abdomen. However, it is feeble and muddled with multiple sources of noise, most notably the Mother's ECG (MECG), whose amplitude is exceptionally high. Several approaches for extracting FECG from signals captured by electrodes implanted on the surface of the mother's body have been proposed in earlier research^[5–8]. However, these approaches necessitate a high number of sensors and are hazardous to the fetus's health when more than two sensors are used^[9–12]. In this article, we propose a new approach by coupling the CNN model with four mathematical tools from the numerical and static analysis: Independent Component Analysis (ICA)^[13], Singular-Value Decomposition (SVD)^[14], Non-negative Matrix Factorization (NMF)^[15], and Empirical Mode Decomposition (EMD)^[16]. These four methods implement different models of the quasi-periodicity of the cardiac signal. The CNN model^[17] exploits the images: spectrograms and scalograms provided by the time-scale and time-frequency analysis of the ECG signal presenting the mixture. In Section 2 of this paper, we will provide the methodology of fetal signal extraction by explaining the general algorithm followed by the fundamental steps implemented to accomplish the objective. Section 3 will give the simulation findings of the proposed approach applying accurate data. In Section 4, the proposed approach's effectiveness, which uses a single sensor and is validated using synthetic data and real recordings, will be discussed and evaluated. Section 5 concludes this paper.

2 Theoretical Background

2.1 Time-Scale Image (TSI)

2.1.1 Continuous Wavelet Transform (CWT)

The CWT^[18, 19] of a signal $x(t)$ is defined as

$$T(a, b) = \frac{1}{\sqrt{a}} \int_{-\infty}^{+\infty} x(t)\Psi^*((t - b)/a) dt \quad (1)$$

where $\Psi^*((t - b)/a)$ is the dilated and translated wavelet.

2.1.2 TSI image conversion

The signal energy's contribution at a particular scale a and location b is

$$\epsilon(a, b) = |T(a, b)|^2 \quad (2)$$

The plot of $\epsilon(a, b)$ presents the scalogram or the TSI.

2.2 SVD

Diagonalizing a matrix is generally very efficient for computing matrix powers. Nevertheless, not all matrices can be diagonalized. Thus, this method cannot be used for rectangular matrices. In certain instances, SVD can substitute diagonalization. SVD permits the separation of a matrix into many orthogonal components^[20]. A matrix M of size $m \times n$ is separated as follows:

$$M = U\Sigma V^T \quad (3)$$

where Σ is a diagonal matrix of size $m \times n$ with positive real coefficients, U and V are two real matrices orthogonal of respective sizes $m \times m$ and $n \times n$, respectively, and "T" denotes the transposition. If we decompose the time-scale image M , the columns u_i of U represent S frequency characteristics, and the columns v_i of V represent the temporal characteristics of S ,

$$\sum_{n=1}^{\min(m,n)} \sigma_{ii} \cdot u_i \cdot v_i^T \quad (4)$$

As a result, M is defined as the sum of uncorrelated models $u_i \cdot v_i^T$, each with an associate amplitude of σ_{ii} . Each frequency characteristic u_i , therefore, corresponds to a characteristic temporal v_i , with the energy σ_{ii}^2 .

2.3 NMF

Let X be an $n \times p$ matrix with only non-negative values and no rows or columns containing just 0; r is a sufficiently small integer chosen in front of n and p . The non-negative factorization of the matrix X is the search for two matrices, $W_{n \times r}$ and $H_{r \times p}$, whose product approaches X and includes only positive or zero values,

$$X \approx W \cdot H \quad (5)$$

Factorization is resolved by obtaining a local maximum of the optimization problem,

$$\min[L(X, W \cdot H) + P(W, H)]_{W, H \geq 0} \quad (6)$$

$L()$ is a loss function evaluating the quality of the approximation, and P is an optional function penalty; $L()$ is typically also a criterion of least squares $L \cdot S$. P is an optional regularization penalty used to force the desired properties of W and H matrices. Let V_{ij} (see Fig. 1) denote the matrix element we want to extract,

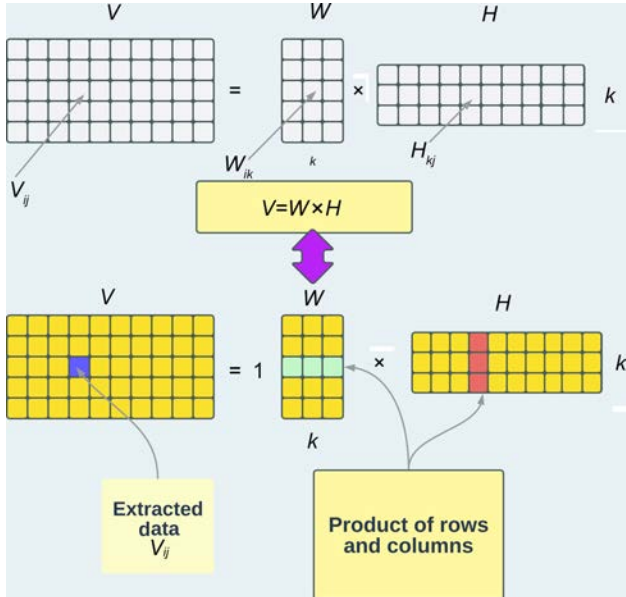


Fig. 1 Extracting data.

and it suffices to build the proper row-column product to extract the needed information^[21].

3 Methodology

3.1 Global algorithm

An electrocardiogram sensor implanted in the mother's abdomen measures a combination of FECG and MECG information (see Fig. 2)^[22]. In mathematical terms, the system is considered indeterminate since the number of sources exceeds the number of observations. Thus we may write

$$X = \alpha \cdot s_F + \beta \cdot s_M + N \quad (7)$$

where both α and β are actual, constant, and non-approaching zero, and

s_F is the FECG;

s_M is the MECG;

X is a mixture of s_F and s_M ; and

N is the noise.

This analysis concentrates primarily on the instantaneous mixture of linear components. Thus, we will overlook the impact of noise N . Consequently, our objective is to identify the sources s_F and s_M .

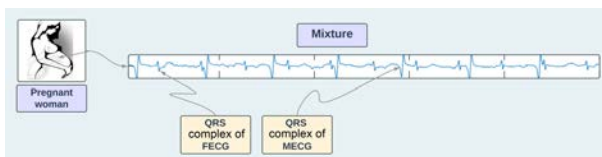


Fig. 2 Mixture signal.

Even though the FECG has a much lower amplitude than MECG, the fetus' cardiac rate is significantly higher. This means that the waves Q , R , and S (QRS complexes) will be located in the time-scale and time-frequency domains using Short-Time Fourier Transform (STFT)^[23] and Continuous Wavelet Transform (CWT) (see Fig. 3). This makes it straightforward to locate all the points that indicate the FECG and MECG. Due to its low amplitude, the fetus's contribution in terms of energy is very low. However, the powerful heartbeat of the fetus makes it easy to illustrate it in the time-frequency and time-scale domains, which is the main focus of this work. In fact, the factorization in NMF enables us to get the exact contributions from both the mother and the fetus. This is done by generating TSI and Time-Frequency Images (TFI), which can be used to build databases with up to 10 000 image data. These images are then fed into CNN networks, which separate the FECG and MECG signals. It is reported that TSI is used in the CNN model, and TFI images are used in the separation process using SVD-ICA methods. So, after capturing a mixture of fetal and maternal electrocardiogram signals, employing surface electrodes placed appropriately on the mother's abdomen. The fetal electrocardiogram is extracted using the following global algorithm (see Fig. 4).

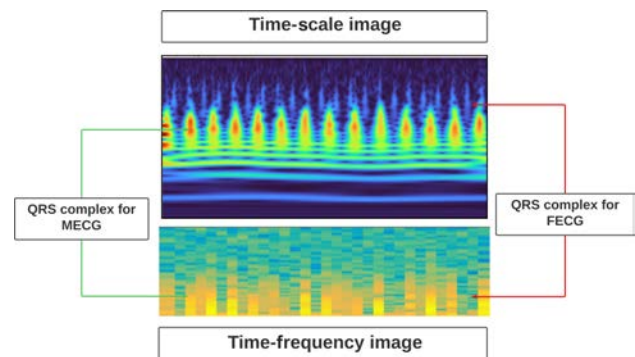


Fig. 3 Time-scale and time-frequency domain of mixture signal.

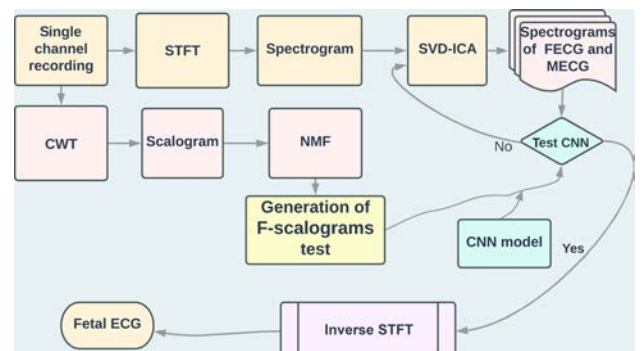


Fig. 4 Representation of global algorithm.

3.2 SVD-ICA for blind source extraction

The proposed model is founded on the equivalency between the studied signal X , its TSI, and its TFI. Dividing the signal into many sources entails separating this TFI and TSI into multiple distinct TFIs and TSIs meant to convey those sources. To provide context for the concept of independence in these surroundings, we must elaborate on underlying assumptions^[23–26]. The TSI is obtained by computing the modulus of a CWT applied to the observed signal $X(t)$. Then, the TSI coefficients are calculated to sort out the amplitude of a specific frequency at a particular time. In the remaining portions of this section, we'll assume that the TSI image is an $m \times n$ matrix (m frequency channels and n time frames). First, TSI is the sum of an unusual number of TSIs. These TSIs are meant to represent the sources,

$$\text{TSI} = \sum_{i=1}^n \text{TSI}_i \quad (8)$$

Second, each TSI_i is mainly composed of the product of a temporal weight vector and a characteristic spectral vector. We can now demonstrate the independence of TSI_i by defining it as the independence of the vectors of correlating spectral characteristics perceived as a sequence of observations of stochastic processes, independent and identically distributed. These are the assertions of the ICA, which is the reason it uses statistical formalism^[27–29]. Figure 5 presents the algorithmic steps of the SVD-ICA model. First, we determine the TSI, denoted M , of a time signal $X(t)$,

$$M = U_n \Sigma_n V_n^T \quad (9)$$

which results from an SVD, where the columns of U_n represent decorrelated spectral characteristics. These

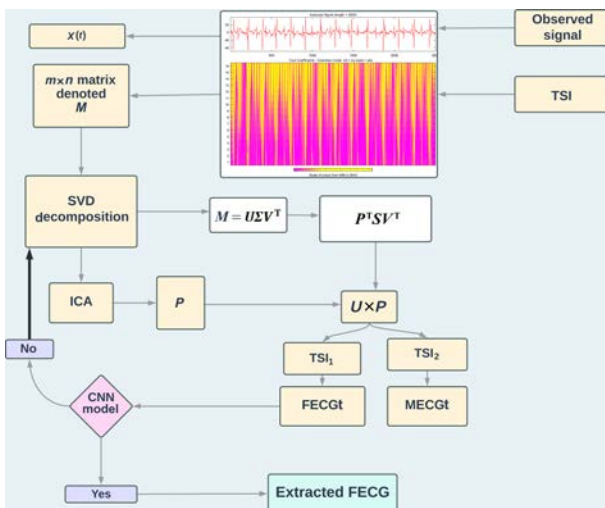


Fig. 5 Algorithmic steps of the SVD-ICA model.

columns are then multiplied by an orthogonal matrix P to ensure maximum independence. The model's notations are as follows:

$$Y_n = V_n P \quad (10)$$

and

$$V_n = U_n \Sigma_n P \quad (11)$$

It is highlighted that, for the SVD, only a handful of frequency and time characteristics, contributing to approximately 99.9% of the signal's energy, are preserved. The MATLAB svd function performs SVD. Whenever the ICA is applied to the columns of U_n , U_n is multiplied by an orthogonal matrix P , such that the columns of $U_n P$ are as independent as possible. The model's hypotheses indicate that the searched separate components are the matrices,

$$\text{TSI}_i = y_i v_i^T \quad (12)$$

where y_i are the columns of $U_n P$ and v_i are those of $V_n \Sigma_n P$. To find the corresponding temporal signals, it is necessary to invert the TSIs using the Inverse Continuous Wavelet Transform (ICWT) algorithms.

3.3 Description of CNN model

As shown in Fig. 6, the original objective of our algorithm is to predict the class of the input ECG images TSI by separating them into two crucial output components: by providing an image as input to the network, it undergoes many convolutions, subsamples, and a completely connected layer before producing output. In the following paragraphs, we discuss the crucial phases in our treatment.

3.3.1 Convolution process

The first step of our approach is the convolution process. In this phase, we will cover feature detectors and

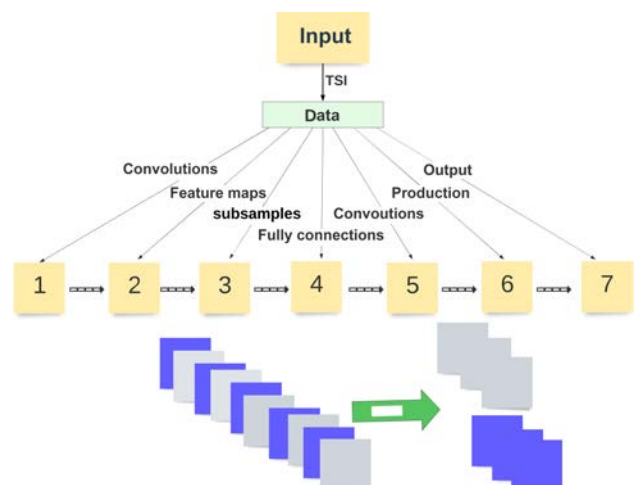


Fig. 6 CNN model.

fundamentally neural network filters. The convolution layer computes the output of neurons connected to local regions or receptive fields in the input, among each neuron generating a linear combination between its weights and the local receptive field to which it is connected in the input volume. So every computation provides a feature map extracted from the input image. Furthermore, we will use Rectified Linear Unit (ReLU) to improve the non-linearity of data images.

3.3.2 Pooling and flattening

Throughout this section, we may explore the maximum pooling that enables the CNN to recognize the image displayed. After completing the previous two phases, we should possess a database of grouped entities. As indicated by the name of this phase, we will flatten our columnar map of features. As shown in Fig. 7, various characteristic cards from the previous step have been joined. After the flattening phase, you have been left with a long vector of input data, which is then transmitted through all the artificial neural networks to be processed.

3.3.3 Full connection

In this phase, the input layer contains the data vector created during the flattening step, which encodes all functionality distilled over the previous stages. They are already perfectly adequate for a high level of accuracy in class recognition at this point. We will now progress to the next degree of intricacy and precision. Establishing a CNN significantly boosts the ability to classify images. The artificial neural network must start by taking this input and integrating the features into a more varied set of properties. In the following section, we would like to compile and import our database to ensure the system can learn the two types of images.

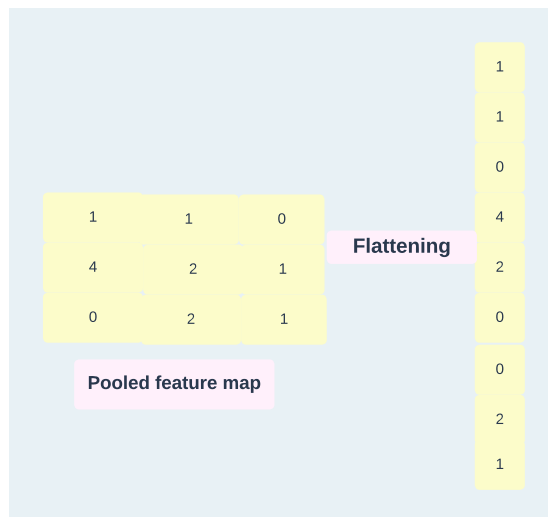


Fig. 7 Characteristic cards.

4 Result and Discussion

4.1 Result

4.1.1 Observed signal

The extraction of the FECG from cutaneous recordings consists of a single channel extracted from the international database Daisy^[30]. We present three signals evaluated from the mother's abdomen, whereas only a single signal is employed in our investigation. The $X(t)$ signal shown in Fig. 8 is a mixture of FECG and MECG signals, with the QRS complexes of each signal being far more distinct despite the FECG's smallish amplitude. We will present the simulation results based on the approach described in this work to determine the MECG and FECG signals. Per the global algorithm (see Fig. 2), we will start with constructing TSIs and the TFIs which thanks to the CWT modules and the STFT. Then we will apply, on the one hand, the NMF methods to generate the target database of the CNN model. On the other hand, the SVD-ICA methods will be applied to create the FECG and MECG signals to be compared with the outputs of the CNN model. All simulations are done on Matlab 2019a and python 5.2.

4.1.2 SVD-ICA methods

Figure 9 shows the results obtained through the model simulation described in Section 3.2.1. It is noted that the SVD-ICA method enables the FECGt and MECGt scalograms to be tested with the CNN model to determine the images closest to reality, and once the test is confirmed, we will proceed to the determination of the ICWT to identify the accurate signals denoted FECGr and MECGr. We also note that all iterations at the SVD-

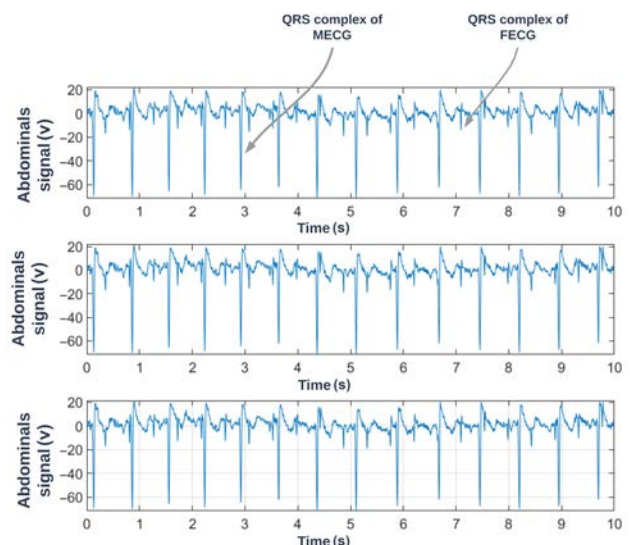


Fig. 8 Observed signals.

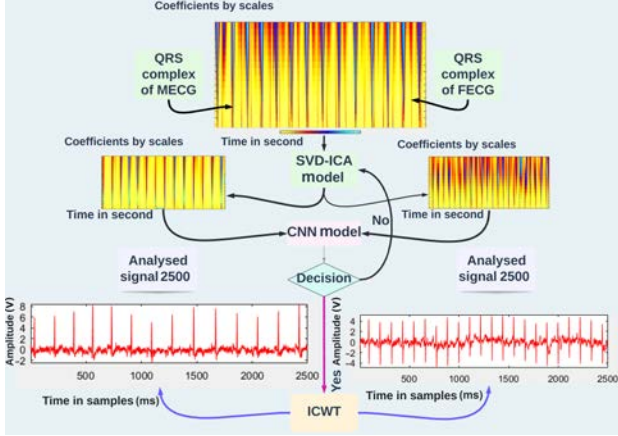


Fig. 9 FECGr and MECGr signals.

ICA algorithm level depend on the independence criteria defining the ICA statistical methods implemented here by the JADE algorithm^[31].

4.1.3 Generation of data

Applying the NMF to the signal $X(t)$, which is considered a matrix, allows us to isolate the fetal QRS complexes from the maternal ones. To establish the required database, we'll next implement a time-scale analysis by shifting the scale from 0.1 to 100 000. The temporal representation of the submatrix $Y(t)$ extracted from $X(t)$ using the NMF is illustrated in Fig. 10. $Y_4(t)$ is the temporal representation of $Y(t)$ after applying the data-adaptive multiresolution technique like Empirical Mode Decomposition (EMD)^[32] of submatrix Y . Therefore, we can generate the required number of TSI images by determining the modulus of CWT of each Y_i . It has been reported that the NMF and EMD tools can be used to generate a mother database consisting of many images used in the CNN test to classify the onrushing shots. The two maternal and fetal databases result from the richness of the wavelet processing. Therefore the nature of the wavelet and the desired scales will change each time. Figure 11 demonstrates a selection of these images. $Z(t)$ is the mother temporal representation of the submatrix related to the MECG and extracted from $X(t)$ using the NMF. The TSI images of FECG and MECG are given in Fig. 12 by using CWT combined with NMF. On a scale from 1 to 10, 1 to 16, 1 to 20, and 1 to 25. The data generated using the “mexh” and “cgau2” wavelets are displayed in Fig. 13.

4.1.4 CNN model

In this, we endeavor to import and compile our database to ensure that the machine can learn to differentiate between the different types of images (Fig. 14a).

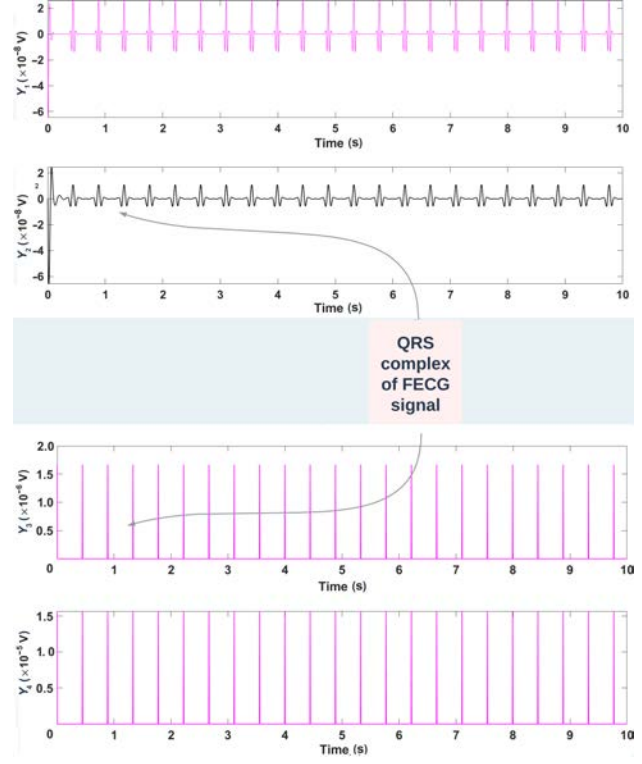


Fig. 10 Submatrix $Y(t)$.

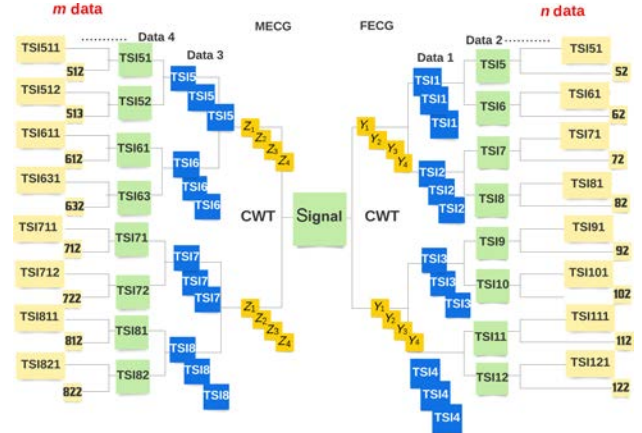


Fig. 11 Model data tree.

Afterwards, our database is separated into two classes (training/test) (Fig. 14b). In the model's training stage, we chose 25 epochs representing a loop that repeats the learning processing of the images over 254 turns. The result is the following (Fig. 14c). The usefulness of our model is then demonstrated by using it to predict the classification of a manufacturer image. Graphs of the findings are shown in Fig. 15. It's a significant improvement over the previous model, allowing for an increased accuracy of 95%. As a last resort, increasing the number of training iterations yields promising outcomes.

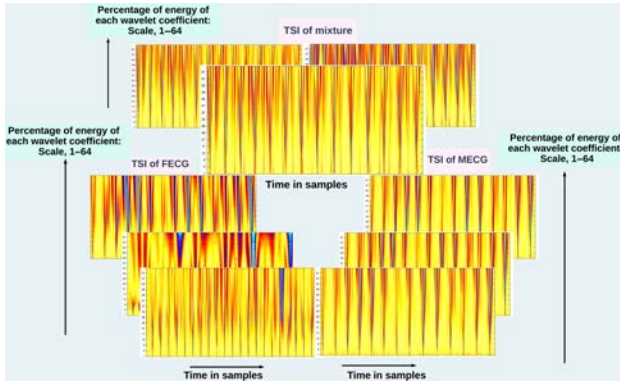


Fig. 12 TSI images of FECG and MECG.

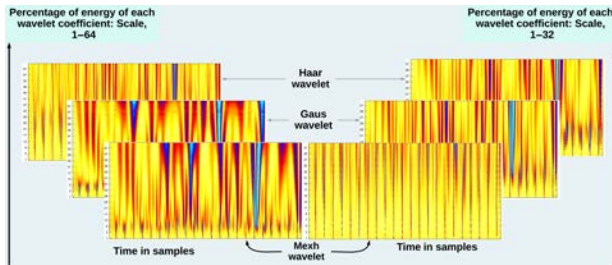


Fig. 13 Data generated using the “mexh” and “cgau2” wavelets.

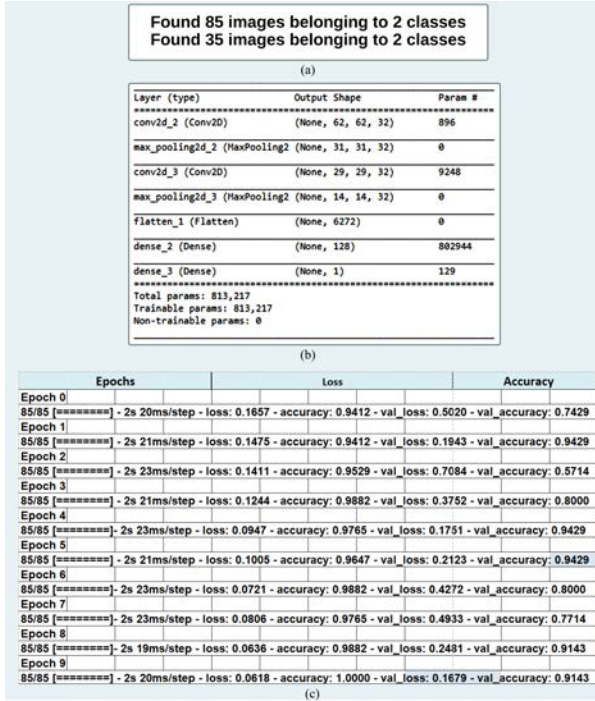


Fig. 14 CNN model results.

4.1.5 Extracted signal FECG

After numerous iterations of SVD-ICA, the CNN algorithm terminates the process when the recognized signal resembles the ideal outcome generated from the CWT-NMF model. Figure 16 provides the optimum

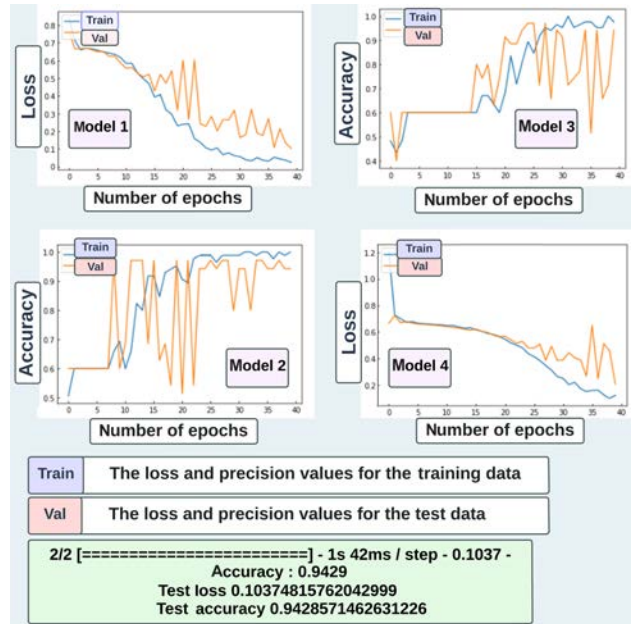


Fig. 15 Loss and accuracy for different models.

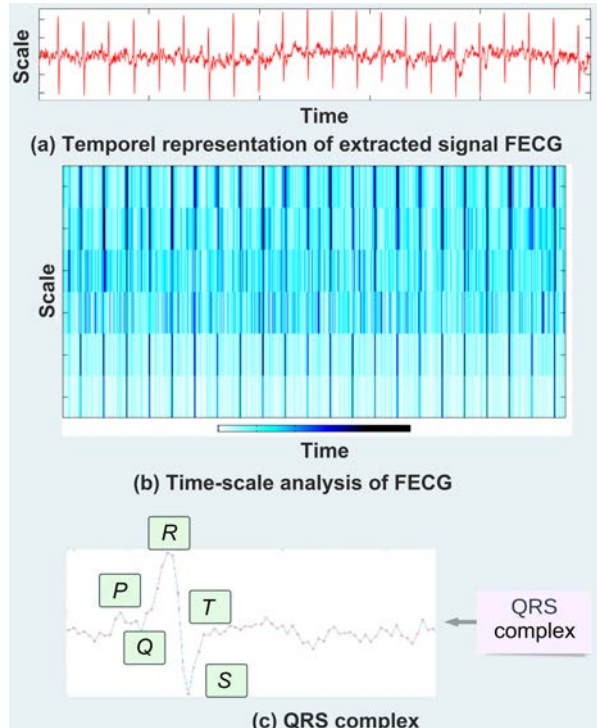


Fig. 16 Extracted signal FECG.

FECG signal. The classification of the fetal QRS complex is depicted in the same diagram.

4.2 Discussion

The methods proposed in this work have provided spectacular results. The extracted FECG signal has an SNR ratio of approximately zero; furthermore, the implementation and programming time is minimal.

Compared with other recent works in the field^[32–36], the presented approach is much more reliable and accurate. On the one hand, the process is based on very subtle mathematics tools that can be developed numerically even for twins and are easily implemented in real-time using embedded systems such as DSP or Raspberry. On the other hand, a remarkable added value of this paper is that it combines the CNN model, one of the most profound algorithms of Deep Learning, with the previous mathematical methods. This tool ensures a comparison with the ideal case and therefore makes it possible to extract an FECG signal as close as possible to reality, which leads to a reliable medical diagnosis based on a single electrode, i.e., from a medical perspective, we will avoid all the risks of using a lot of sensors to the health of the mother and her fetus that come from the cables, current waves, and electric tension. It is also noted that the data used in the CNN model is self-generated, can range into millions, and can be used by any researcher or academic. Another database can be generated using the time-frequency analysis based on the STFT tool. Figure 17 shows the time-frequency images formed by the STFT tool, subdivided by the SVD-ICA algorithm, and spread out to millions by varying the properties of the window, its width, nonequispaced fast Fourier transforms, and the overlap using the spectrum function on Matlab.

The CNN model has demonstrated its efficiency through the results and graphs, which compare the accuracy values to the loss values and demonstrate that the model has a 94% performance level. This study may

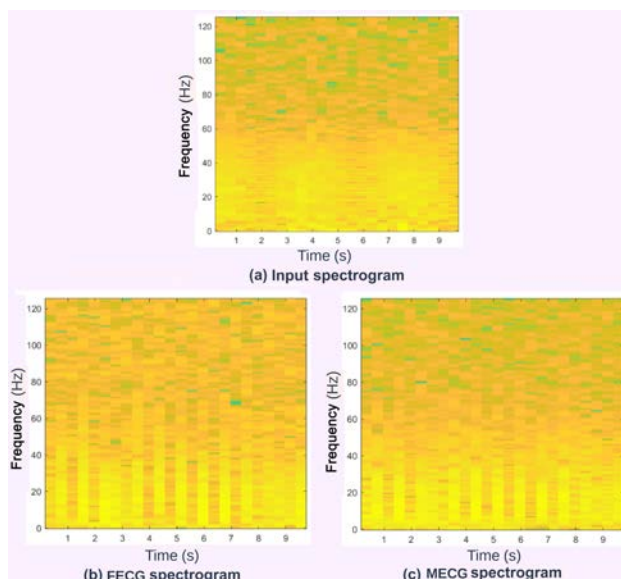


Fig. 17 FECG and MECG spectrograms.

benefit us in expanding to a subsequent perceptual level, such as separation using the K-means model.

The undeniable value of wavelets in biomedical engineering is highlighted in this work. Additionally, it is mentioned that this mathematical tool can be applied to energy^[37–39] and motor control^[40,41] for electric vehicles.

5 Conclusion

This paper introduces an innovative approach for processing biomedical signals, especially for monitoring the fetal heartbeat using a single electrode implanted in the mother's abdomen. This research investigated various mathematical algorithms, including ICA, SVD, NMF, and EMD. The exciting aspect of our investigation is the incorporation of artificial intelligence, notably the CNN algorithm as a filtering and classification algorithm, to assist us in identifying the temporal signal associated with fetal electrical activity. It has been reported that the invested model can also work effectively for twins by simply increasing the number of epochs. Effectiveness is proven by the optimal processing time of the developed algorithms and the reliability of the reconstructed signal. This reveals the potential for exploiting the proposed approaches in cardiology and cardiopedia, given that 1 out of 125 newborns die each year due to heart defects that begin sadly in the first weeks of pregnancy and can be easily identified and handled if we can recover to the fetal electrocardiogram signal. This model allows cardiologists to check for these irregularities in real-time from a flying lab. Subsequently, this paper lays the groundwork for researchers to integrate artificial intelligence systems into the field of statistical learning and signal processing, which involves the challenges of data processing and big data.

References

- [1] W. Samek, G. Montavon, S. Lapuschkin, C. J. Anders, and K. R. Müller, Explaining deep neural networks and beyond: A review of methods and applications, *Proc. IEEE*, vol. 109, no. 3, pp. 247–278, 2021.
- [2] M. Fetanat, M. Stevens, P. Jain, C. Hayward, E. Meijering, and N. H. Lovell, Fully Elman neural network: A novel deep recurrent neural network optimized by an improved Harris hawks algorithm for classification of pulmonary arterial wedge pressure, *IEEE Trans. Biomed. Eng.*, vol. 69, no. 5, pp. 1733–1744, 2022.
- [3] Z. Gao, Z. Lu, J. Wang, S. Ying, and J. Shi, A convolutional neural network and graph convolutional network based framework for classification of breast histopathological images, *IEEE J. Biomed. Health Inf.*, vol. 26, no. 7, pp.

- 3163–3173, 2022.
- [4] M. Wang, K. C. M. Lee, B. M. F. Chung, S. V. Bogaraju, H. C. Ng, J. S. J. Wong, H. C. Shum, K. K. Tsia, and H. K. H. So, Low-latency in situ image analytics with FPGA-based quantized convolutional neural network, *IEEE Trans. Neural Netw. Learn. Syst.*, vol. 33, no. 7, pp. 2853–2866, 2022.
 - [5] S. Ziani, A. Jbari, L. Bellarbi, and Y. Farhaoui, Blind maternal-fetal ECG separation based on the time-scale image TSI and SVD-ICA methods, *Procedia Comput. Sci.*, vol. 134, pp. 322–327, 2018.
 - [6] S. Ziani, Y. El Hassouani, and Y. Farhaoui, An NMF based method for detecting RR interval, in *Proc. 2019 Int. Conf. on Big Data and Smart Digital Environment*, Casablanca, Morocco, 2019, pp. 342–346.
 - [7] S. Ziani and Y. El Hassouani, Fetal-maternal electrocardiograms mixtures characterization based on time analysis, in *Proc. 5th Int. Conf. on Optimization and Applications (ICOA)*, Kenitra, Morocco, 2019, pp. 1–5.
 - [8] A. D. C. Chan, M. M. Hamdy, A. Badre, and V. Badee, Wavelet distance measure for person identification using electrocardiograms, *IEEE Trans. Instrum. Meas.*, vol. 57, no. 2, pp. 248–253, 2008.
 - [9] S. Ziani and Y. El Hassouani, Fetal electrocardiogram analysis based on LMS adaptive filtering and complex continuous wavelet 1-D, in *Proc. 3rd Int. Conf. on Big Data and Networks Technologies*, Leuven, Belgium, 2020, pp. 360–366.
 - [10] A. Hyvarinen, Blind source separation by nonstationarity of variance: A cumulant-based approach, *IEEE Trans. Neural Netw.*, vol. 12, no. 6, pp. 1471–1474, 2001.
 - [11] L. Parra and C. Spence, Convulsive blind separation of non-stationary sources, *IEEE Trans. Speech Audio Process.*, vol. 8, no. 3, pp. 320–327, 2000.
 - [12] D. T. Pham and J. F. Cardoso, Blind separation of instantaneous mixtures of non-stationary sources, *IEEE Trans. Signal Process.*, vol. 48, no. 2, pp. 363–375.
 - [13] J. F. Cardoso, Infomax and maximum likelihood for blind source separation, *IEEE Signal Process. Lett.*, vol. 4, no. 4, pp. 112–114, 1997.
 - [14] P. P. Kanjilal, S. Palit, and G. Saha, Fetal ECG extraction from single-channel maternal ECG using singular value decomposition, *IEEE Trans. Biomed. Eng.*, vol. 44, no. 1, pp. 51–59, 1997.
 - [15] Y. X. Wang and Y. J. Zhang, Nonnegative matrix factorization: A comprehensive review, *IEEE Trans. Knowl. Data Eng.*, vol. 25, no. 6, pp. 1336–1353, 2013.
 - [16] H. Wei, T. Qi, G. Feng, and H. Jiang, Comparative research on noise reduction of transient electromagnetic signals based on empirical mode decomposition and variational mode decomposition, *Radio Sci.*, vol. 56, no. 10, p. e2020RS007135, 2021.
 - [17] D. Kollias and S. Zafeiriou, Exploiting multi-CNN features in CNN-RNN based dimensional emotion recognition on the OMG in-the-wild dataset, *IEEE Trans. Affect. Comput.*, vol. 12, no. 3, pp. 595–606, 2021.
 - [18] S. Ziani, A. Jbari, and L. Bellarbi, Fetal electrocardiogram characterization by using only the continuous wavelet transform CWT, in *Proc. 2017 Int. Conf. on Electrical and Information Technologies (ICEIT)*, Rabat, Morocco, 2017, pp. 1–6.
 - [19] T. Guo, T. Zhang, E. Lim, M. López-Benítez, F. Ma, and L. Yu, A review of wavelet analysis and its applications: Challenges and opportunities, *IEEE Access*, vol. 10, pp. 58869–58903, 2022.
 - [20] B. Lei, I. Y. Soon, and E. L. Tan, Robust SVD-based audio watermarking scheme with differential evolution optimization, *IEEE Trans. Audio, Speech, Lang. Process.*, vol. 21, no. 11, pp. 2368–2378, 2013.
 - [21] S. Ziani, A. Jbari, and L. Bellarbi, QRS complex characterization based on non-negative matrix factorization NMF, in *Proc. 4th Int. Conf. on Optimization and Applications (ICOA)*, Mohammedia, Morocco, 2018, pp. 1–5.
 - [22] L. Su and H. T. Wu, Extract fetal ECG from single-lead abdominal ECG by de-shape short time Fourier transform and nonlocal median, *Front. Appl. Math. Stat.*, vol. 3, p. 2, 2017.
 - [23] N. Q. K. Duong, E. Vincent, and R. Gribonval, Under-determined convulsive blind source separation using spatial covariance models, in *Proc. 2010 IEEE Int. Conf. on Acoustics, Speech and Signal Processing*, Dallas, TX, USA, 2010, pp. 9–12.
 - [24] S. Sargolzaei, K. Faez, and A. Sargolzaei, Signal processing based for fetal electrocardiogram extraction, in *Proc. 2008 Int. Conf. on BioMedical Engineering and Informatics*, Sanya, China, 2008, pp. 492–496.
 - [25] M. S. Vadivu and M. Kavithaa, A novel fetal ECG signal extraction from maternal ECG signal using conditional generative adversarial networks (CGAN), *J. Intell. Fuzzy Syst.*, vol. 43, no. 1, pp. 801–811, 2022.
 - [26] X. Pu, L. Long, L. Han, M. Ding, and J. Peng, Hybrid method based on extreme learning machine for fetal electrocardiogram extraction, in *Proc. 14th Int. Conf. on Communication Software and Networks (ICCSN)*, Chongqing, China, 2022, pp. 105–108.
 - [27] R. Martinek, R. Kahankova, J. Jezewski, R. Jaros, J. Mohylova, M. Fajkus, J. Nedoma, P. Janku, and H. Nazeran, Comparative effectiveness of ICA and PCA in extraction of fetal ECG from abdominal signals: Toward non-invasive fetal monitoring, *Front. Physiol.*, vol. 9, p. 648, 2018.
 - [28] R. Sameni, C. Jutten, and M. B. Shamsollahi, What ICA provides for ECG processing: Application to noninvasive fetal ECG extraction, in *Proc. 2006 IEEE Int. Symp. on Signal Processing and Information Technology*, Vancouver, Canada, 2006, pp. 656–661.
 - [29] V. D. Vrable and J. I. Mars, SVD-ICA: A new tool to enhance the separation between signal and noise subspaces, in *Proc. 11th European Signal Processing Conf.*, Toulouse, France, 2002, pp. 1–4.
 - [30] B. De Moor, P. De Gersem, B. De Schutter, and W. Favoreel, DAISY: A database for identification of systems, *J. A.*, vol. 38, no. 4, p. 5, 1997.
 - [31] S. B. Sadkhan, S. J. Mohammed, and M. M. Shubbar,

- Fast ICA and JADE algorithms for DS-CDMA, in *Proc. 2nd Al-Sadiq Int. Conf. on Multidisciplinary in IT and Communication Science and Applications (AIC-MITCSA)*, Baghdad, Iraq, 2017, pp. 325–329.
- [32] Z. Said and Y. El Hassouani, A new approach for extracting and characterizing fetal electrocardiogram, *Trait. Signal*, vol. 37, no. 3, pp. 379–386, 2020.
- [33] F. Ghayem, B. Rivet, R. C. Farias, and C. Jutten, Robust sensor placement for signal extraction, *IEEE Trans. Signal Process.*, vol. 69, pp. 4513–4528, 2021.
- [34] M. R. Mohebbian, S. S. Vedaei, K. A. Wahid, A. Dinh, H. R. Marateb, and K. Tavakolian, Fetal ECG extraction from maternal ECG using attention-based CycleGAN, *IEEE J. Biomed. Health Inf.*, vol. 26, no. 2, pp. 515–526, 2022.
- [35] D. Jilani, T. Le, T. Etchells, M. P. H. Lau, and H. Cao, Lullaby: A novel algorithm to extract fetal QRS in real time using periodic trend feature, *IEEE Sensors Lett.*, vol. 6, no. 9, p. 7003204, 2022.
- [36] R. Jaros, R. Martinek, R. Kahankova, and J. Koziorek, Novel hybrid extraction systems for fetal heart rate variability monitoring based on non-invasive fetal electrocardiogram, *IEEE Access*, vol. 7, pp. 131758–131784, 2019.
- [37] M. Ouhadou, A. El Amrani, C. Messaoudi, and S. Ziani, Experimental investigation on thermal performances of SMD LEDs light bar: Junction-to-case thermal resistance and junction temperature estimation, *Optik*, vol. 182, pp. 580–586, 2019.
- [38] M. Ouhadou, A. El Amrani, S. Ziani, and C. Messaoudi, Experimental modeling of the thermal resistance of the heat sink dedicated to SMD LEDs passive cooling, in *Proc. 3rd Int. Conf. on Smart City Applications*, Tetouan, Morocco, 2018, p. 30.
- [39] I. Laabab, S. Ziani, and A. Benami, Solar panels overheating protection: A review, *Indones. J. Electr. Eng. Comput. Sci.*, vol. 29, no. 1, pp. 49–55, 2023.
- [40] H. B. Achour, S. Ziani, Y. Chaou, Y. El Hassouani, and A. Daoudia, Permanent magnet synchronous motor PMSM control by combining vector and pi controller, *WSEAS Trans. Syst. Control*, vol. 17, pp. 244–249, 2022.
- [41] Y. Chaou, S. Ziani, H. B. Achour, and A. Daoudia, Nonlinear control of the permanent magnet synchronous motor PMSM using backstepping method, *WSEAS Trans. Syst. Control*, vol. 17, pp. 56–61, 2022.



Said Ziani is a professor at University of Hassan II, Casablanca, Morocco. His research interests include digital design, industrial applications, industrial electronics, industrial informatics, power electronics, motor drives, renewable energy, FPGA and DSP applications, embedded systems, adaptive control, neural network control, automatic robot control, motion control, and artificial intelligence. He is a senior member of IEEE.



Mohammed Moutaib is a PhD candidate at the University of Moulay Ismail (UMI), Meknes, Morocco. He received the MEng degree in big data and Internet of objects from the University of Hassan II, Casablanca, Morocco in 2019. Currently, his research interests include learning, e-learning, computer security, big data analytics, and business intelligence.



Yousef Farhaoui is a professor at Moulay Ismail University of Meknes, Morocco. He is the chair of IDMS Team, director of the STI Laboratory, and the local publishing and research coordinator of Cambridge International Academics in United Kingdom. He received the PhD degree in computer security from Ibn Zohr University of Science. His research interests include learning, e-learning, computer security, big data analytics, and business intelligence. He is a senior member of IEEE, IET, ACM, and EAI Research Group.